Biochemical and Biophysical Research Communications 463 (2015) 994–998

Contents lists available at ScienceDirect

Biochemical and Biophysical Research Communications

journal homepage: www.elsevier.com/locate/ybbrc

The *Caenorhabditis elegans R13A5.9* gene plays a role in synaptic vesicle exocytosis

Tarou Ogurusu*, Kazumi Sakata, Tokumitsu Wakabayashi, Yutaro Shimizu, Ryuzo Shingai

Department of Chemistry and Bioengineering, Iwate University, 4 Ueda, Morioka, Iwate 020-8551, Japan

ARTICLE INFO

Article history:
Received 28 May 2015
Accepted 7 June 2015
Available online 12 June 2015

Keywords:
R13A5.9
C. elegans
Synaptic vesicle exocytosis
Aldicarb resistance

ABSTRACT

The *Caenorhabditis elegans R13A5.9* gene encodes a putative membrane protein with homologs in mammals. When the R13A5.9 protein was fused to different fluorescent proteins, signal was observed in or near synaptic vesicles; thus, we sought to determine whether this gene plays a role in synaptic vesicle formation, function, or exocytosis. *R13A5.9* mutant worms exhibited low sensitivity to aldicarb (an acetylcholinesterase inhibitor), which suggested that vesicular loading or release, or acetylcholine synthesis, was disrupted in these organisms. This was supported by the observation that an *R13A5.9* mutant strain exhibited an excessive accumulation of synaptic vesicles. Collectively, these results suggest a functional role for R13A5.9 in synaptic vesicle exocytosis.

© 2015 Elsevier Inc. All rights reserved.

1. Introduction

The nematode *Caenorhabditis elegans* is a model organism commonly used in developmental biology and neurology research. Its genomic sequence has been available since 1998 [1], which has proven invaluable for the study of gene function. Many *C. elegans* genes of unknown function exist, and have highly conserved homologs in mammals, indicating that these genes possess important roles [1]. We aimed to characterize such "unknown" genes expressed in *C. elegans* neurons, in order to understand the roles their products play in the nervous system. Several known neuronal genes are included in three groups of coregulated genes: mount 1, mount 6, and mount 13 [2]. Previously, we selected conserved genes with unknown function from each of these three groups and examined their expression patterns by using green fluorescent protein (GFP) as a reporter. We identified one gene belonging to mount 6, *R13A5.9*, which demonstrated neural expression (Ogurusu et al., 2006, Synaptic expression of *R13A5.9* gene product in *C. elegans*, 2P-A-360, 11th FAOBMB Congress). The *R13A5.9* encodes a putative membrane protein comprised of 630 amino acids (GenBank idenfier gi: 17554606, see Supplementary Fig. 1), and a BLAST search conducted with this predicted amino acid sequence revealed BLST score matches with many metazoan proteins including mouse and human homologs (367 bits for gi: 157134775 "*Aedes aegypti*", 310 bits for gi: 74005084 "*Canis lupus familiaris*", 308 bits for gi: 148230170 "*Sus sucrofa*", 301 bits for gi: 612020145 "*Monodelphis domestica*", 300 bits for gi: 30017395 "*Mus musculus*", 297 bits for gi: 564368304 "*Rattus norvegicus*", 296 bits for gi: 114582278 "*Pan troglodytes*", 293 bits for gi: 528900366 "*Bos taurus*", 292 bits for gi: 144953907 "*Homo sapiens*", 290 bits for gi: 513192627 "*Gallus gallus*"), but no clear yeast homologs were obtained. These metazoan homologs may have a similar function.

As our study assessing *R13A5.9* expression suggested a possible neural role for this gene, in the present study we sought to further characterize the localization and function of R13A5.9. It was found that R13A5.9 is expressed within, or in close proximity to, synaptic vesicles in *C. elegans*. Furthermore, mutant *R13A5.9* worms demonstrated low sensitivity to the nematicide aldicarb (an acetylcholinesterase inhibitor) and the excessive accumulation of synaptic vesicles. Collectively, our results suggest that R13A5.9 plays a role in synaptic vesicle exocytosis in *C. elegans.*

2. Materials and methods

2.1. Strains

The following strains were obtained from the *C. elegans* Genetic Center (CGC; University of Minnesota, MN, USA): wild-type Bristol N2, CZ333 *juIs1*[*unc-25*p:SNB-1:GFP] IV, levamisole-resistant CB211 *lev-1*(*e211*) IV, aldicarb-resistant RM956 *ric-4*(*md1088*) V, aldicarb-resistant MF200 *ric-3*(*hm9*) IV, and VC2651 *R13A5.9*(*ok3373*) III.

* Corresponding author.
E-mail address: ogurusu@iwate-u.ac.jp (T. Ogurusu).

http://dx.doi.org/10.1016/j.bbrc.2015.06.048
0006-291X/© 2015 Elsevier Inc. All rights reserved.

2.2. Isolation of an R13A5.9 mutant

To isolate *R13A5.9* mutants, synchronized L4 larvae or young adults were treated with trimethylpsoralen and UV light to induce deletion mutations, as previously described [3]. Approximately 600,000 genomes were screened using nested PCR (for information on PCR primers, see Supplementary Table 1) [4], and one deletion mutant was obtained.

2.3. Treatment of C. elegans with aldicarb or levamisole

Groups of approximately 100–150 adult worms (N2, CB211, MF200, RM956, or *R13A5.9* mutants) were incubated with different concentrations of levamisole (0.06 mM, 0.12 mM, 0.25 mM, 0.5 mM) (TCI, Japan) or aldicarb (0.25 μg/mL, 50 μg/mL, 100 μg/mL, and 200 μg/mL) (AccuStandard, CT, USA) for 3 h at 20 °C in 50 mm dishes. Worms that did not move for 3 min were regarded as paralyzed.

2.4. DNA amplification, plasmids, and creation of expression constructs

DNA fragments were amplified using high-fidelity PCR with KOD-plus DNA polymerase (Toyobo, Japan) (for PCR primers, see Supplementary Table 1), and were inserted into plasmid vectors using MultiSite Gateway technology (Invitrogen, CA, USA). The GFP and *Discosoma* sp. monomeric red fluorescent protein (DsRed-Monomer) genes were amplified using the *C. elegans* GFP vector pPD95.67 (a gift from Andrew Fire, Stanford University, CA, USA) and pDsRed-Monomer (Clontech, CA, USA) as templates, respectively. These DNA fragments were cloned into pDONR221 (Invitrogen), and the nuclear localization signal sequence inserted at the *Kpn*I site of the GFP gene was removed from the vector. The 3′ element containing the 3′-UTR sequences was amplified using pPD95.67 as a template, and then cloned into pDONR P2R–P3 (Invitrogen).

In order to construct transgenes encoding R13A5.9 fused to GFP or DsRed-Monomer under the control of the *R13A5.9* promoter, we amplified the 5′ element of *R13A5.9* using worm genomic DNA as a template. Similarly, in order to construct a transgene encoding synaptobrevin/SNB-1 [5] and DsRed-Monomer (p*snb-1*:SNB-1:DsRed-Monomer), the 5′ element of *snb-1* was amplified using worm genomic DNA as a template. These DNA fragments were cloned into pDONR P4–P1R (Invitrogen). The R13A5.9-GFP-3′-UTR, R13A5.9-DsRed-Monomer-3′-UTR, and SNB-1-DsRed-Monomer-3′-UTR expression constructs were created by conducting *att*L-*att*R (LR) recombination reactions between the entry vectors and pDEST R4-R3. Germline transformations were performed as previously described by injecting 50 ng/μL of test DNA into the gonads of wild type (N2), CZ333, or *R13A5.9* mutant worms [6].

2.5. Microscopy

Live worms were mounted on 2% agarose pads containing 10 mM levamisole. We then obtained fluorescent and DIC images using either a fluorescence microscope (Axioskop 2 Plus, Carl Zeiss, Germany), spinning disk confocal microscope (BX-DSU, Olympus, Japan), or laser scanning confocal microscope (C2Si, Nikon, Japan). Images were analyzed with ImageJ software (National Institutes of Health, MD, USA).

2.6. Statistical analysis

The values were expressed as mean ± standard deviation, and differences between groups were determined using an unpaired *t*-test. The significance level for difference for all tests was P value less than 0.05.

3. Results

3.1. Expression of R13A5.9 in or near synaptic vesicles

R13A5.9 fused with GFP (R13A5.9:GFP) was expressed in N2 worms under the control of the *R13A5.9* promoter to visualize the localization of R13A5.9. Distinct punctate fluorescence was primarily localized to the synaptic regions in the nerve ring, ventral nerve cord, and tail. In addition, weak signal was occasionally observed in adult intestinal cells (data not shown). To further elucidate the subcellular localization of R13A5.9 in neurons, a synaptic vesicle protein (SNB-1) fused with DsRed-Monomer (SNB-1:DsRed-Monomer) was co-expressed under the control of the *snb-1* promoter. It was reported that SNB-1 was expressed in vast majority of all neurons [7]. GFP and DsRed-Monomer signals overlapped extensively in the nerve ring, ventral nerve cord, and tail neurons (Fig. 1A–C). Spinning disk confocal microscopy demonstrated co-localization of R13A5.9:GFP with SNB-1:DsRed-Monomer in dorsal nerve cord (Fig. 1D). These results suggested the synaptic localization of R13A5.9 in vast majority of all neurons. To examine expression of R13A5.9 in synaptic vesicles, we expressed R13A5.9 fused with DsRed-Monomer (R13A5.9:DsRed-Monomer) in CZ333 worms which stably expressed SNB-1:GFP in presynaptic terminals of GABAergic DD and VD motor neurons, and in RME neurons, and were used to examine the distribution of synaptic vesicles [8,9]. Resulting R13A5.9:DsRed-Monomer and SNB-1:GFP signals were examined using a laser scanning confocal microscope (Fig. 1E). Quantitative colocalization analysis showed intermediate correlation between the expressions of SNB-1:GFP and R13A5.9:DsRed-Monomer, suggesting that R13A5.9 is present in or near synaptic vesicles.

3.2. Phenotypes of R13A5.9 mutant worms, including low sensitivity to aldicarb

We isolated an *R13A5.9* mutant with a 1.2 kb deletion in the *R13A5.9* gene (Supplementary Fig. 1). This deletion results in a frameshift at residue 54, which yields a premature stop codon at residue 83, suggesting that our *R13A5.9* mutation is a loss-of-function mutation. The isolated mutant was outcrossed seven times and designated as TOG1; TOG1 worms exhibited reduced brood size, low hatch rate, low viability of larvae, slow movement, and an accumulation of large vacuoles in intestinal cells. The frequency of lateral swimming movements of the TOG1 worms (104 ± 35 movements/min, n = 36) in M9 solution [10] was significantly lower ($P = 2.9 \times 10^{-23}$) than that observed in wild-type (N2) worms (215 ± 23 movements/min, n = 36). Slow movement and other mutant phenotypes were rescued by the expression of R13A5.9:GFP in TOG1 worms.

Given the synaptic localization of R13A5.9:GFP (Fig. 1) and slow movement of TOG1 worms, we speculated that R13A5.9 plays a role in synapse function. To investigate this, we compared the cholinergic pharmacology of TOG1 and wild-type worms. Levamisole is a potent cholinergic agonist, and levamisole treatment leads to the hypercontracted paralysis of worms [11]. Acetylcholine reception and postsynaptic response appeared normal in TOG1 worms, as these worms were sensitive to levamisole (Fig. 2A). In contrast, TOG1 worms showed low sensitivity to aldicarb (Fig. 2B). At 200 μg/mL aldicarb, the percentage of paralyzed TOG1 worms (34 ± 10%) was significantly smaller ($P = 0.0044$) than that of wild-type (N2) worms (93 ± 4%). Normally, aldicarb inhibits acetylcholinesterase in wild-type worms, leading to the buildup of acetylcholine at

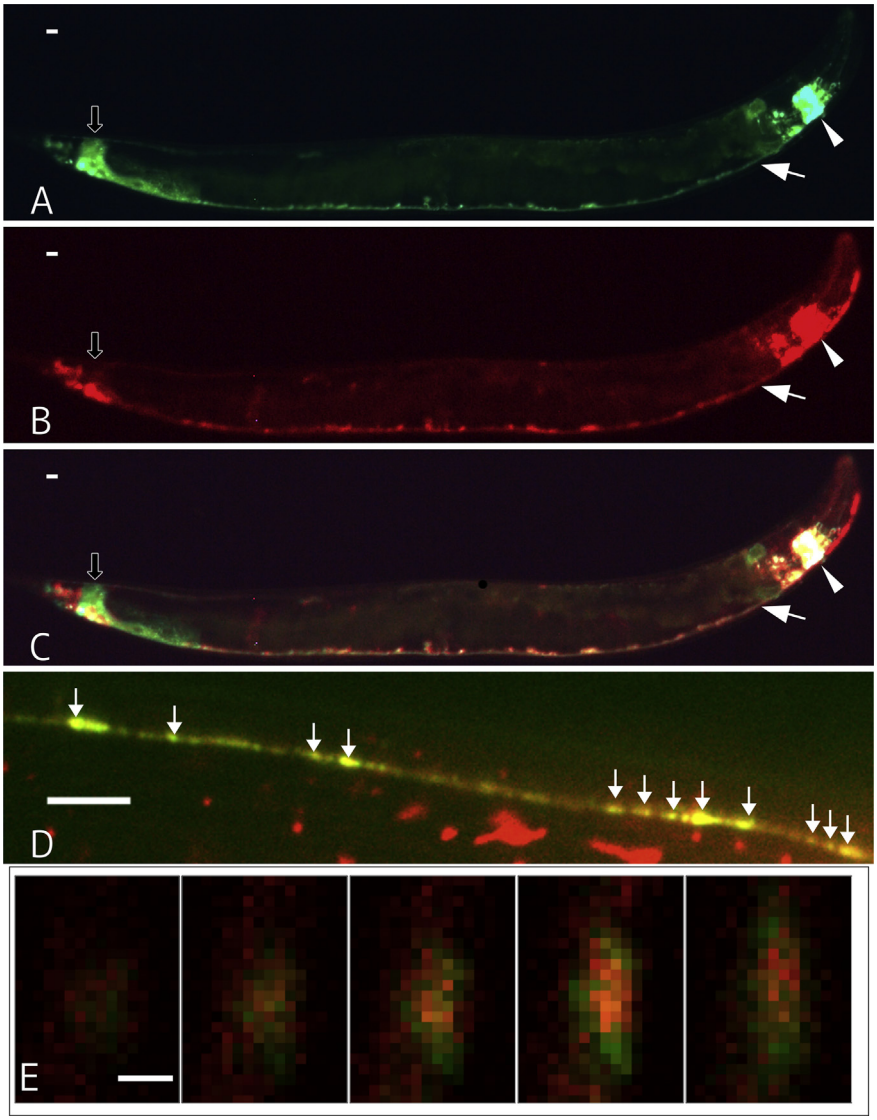

Fig. 1. Expression of R13A5.9 in synaptic regions. (A–C) Co-localization of R13A5.9:GFP with synaptic vesicle marker SNB-1:DsRed-Monomer in the nerve ring (white arrow head), ventral nerve cord (white arrow), and tail neurons (black arrow). (A) GFP image. (B) DsRed-Monomer fluorescence image of the same field in (A). (C) merged image of (A) and (B). (D) Spinning disk confocal image of R13A5.9:GFP (green) expression superimposed on an image of SNB-1:DsRed-Monomer (red) expression; co-localization occurs in the dorsal nerve cord (white arrows). (E) Confocal images of a synapse in a dorsal nerve cord were collected at 0.2 μm intervals in the z axis. Confocal images of R13A5.9:DsRed-Monomer (red) expression were superimposed on those of SNB-1:GFP (green) expression; co-localization was examined using an ImageJ plugin (Colocalization Analysis, Wright Cell Imaging Facility, Canada). From left to right, Pearson's correlation coefficients were as follows: 0.68, 0.74, 0.74, 0.68, and 0.52. Scale bars in (A–C) represent 10 μm; scale bars in (D) and (E) represent 5 μm and 1 μm, respectively.

neuromuscular junctions and hypercontracted paralysis [12]. Disrupted acetylcholine synthesis, or abnormal vesicular loading or release, could explain the low sensitivity of TOG1 worms to aldicarb [7,13,14].

To examine mutant phenotypes further, another *R13A5.9* mutant strain VC2651 was obtained from CGC and outcrossed seven times. A 518 bp deletion in the *R13A5.9* gene of VC2651 results in a frameshift at residue 164, which yields a premature stop codon at residue 177 (Supplementary Fig. 1). The population growth rate and the frequency of lateral swimming movements in M9 solution of VC2651 worms were somewhat slower than those observed in wild-type worms. In addition, VC2651 worms showed a less pronounced but significant ($P = 0.03$ at 100 μg/mL aldicarb) resistance to aldicarb (Fig. 2B). These mild phenotypes of VC2651 worms could be due to residual function of the mutant R13A5.9 which was 94 residues longer than that of TOG1 worms.

3.3. Excessive accumulation of synaptic vesicles in R13A5.9 mutant (TOG1) worms

To examine the functional role of R13A5.9, we observed synaptic vesicles in TOG1 worms, which showed distinctive phenotypes. Fluorescence from SNB-1:GFP, introduced into TOG1 worms by crossing them to CZ333 worms (CZ333 × TOG1 worms), was recorded using a fluorescent microscope. At the dorsal nerve cord in the midbody, the fluorescence intensity per synapse of CZ333 × TOG1 worms (37 ± 39 AU, n = 48) was significantly stronger ($P = 0.0028$) than that of CZ333 worms (18 ± 15 AU, n = 55). These results suggested an excessive accumulation of synaptic vesicles in *R13A5.9* mutant worms. For quantitative comparison of the spatial distribution of synaptic vesicles in CZ333 and CZ333 × TOG1 worms, fluorescent signals were observed using a laser scanning confocal microscope (Fig. 3A and B). The spatial

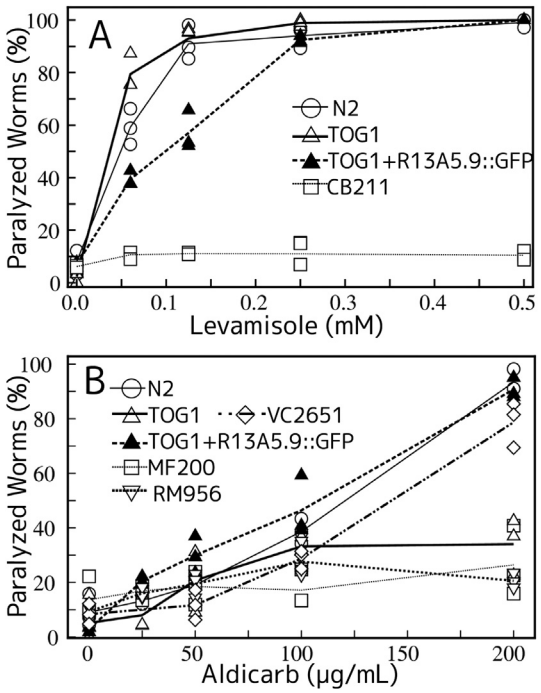

Fig. 2. Low sensitivity of R13A5.9 mutants to aldicarb. Paralysis of adult N2 (open circles), levamisole-resistant CB211 (open squares, A only), aldicarb-resistant MF200 (open squares, B only), aldicarb-resistant RM956 (open reverse triangles, B only), TOG1 (open triangles), TOG1 transformed with R13A5.9:GFP (closed triangles), and VC2651 (open diamonds, B only) worms treated with levamisole (A) or aldicarb (B).

distribution of synaptic vesicles in CZ333 × TOG1 worms was distinct from that of CZ333 worms (Fig. 3C), as evidenced by the fact that the full width at half maximum of fluorescent signal perpendicular to the dorsal nerve cord of CZ333 × TOG1 worms (1.0 ± 0.25 μm, n = 76) was significantly wider ($P = 5.3 \times 10^{-77}$) than that of CZ333 worms (0.54 ± 0.12 μm, n = 75). Furthermore, the fluorescence peak intensity of CZ333 × TOG1 worms (1000 ± 540 AU, n = 76) was significantly stronger ($P = 5.7 \times 10^{-8}$)

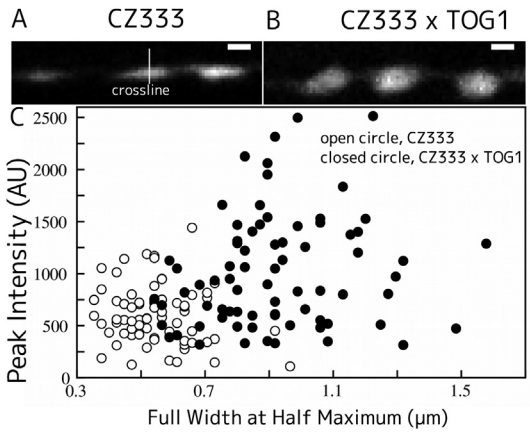

Fig. 3. Distribution of synaptic vesicles in the dorsal nerve cords of R13A5.9 mutant (CZ333 × TOG1) worms. Laser confocal images of dorsal nerve cords expressing SNB-1:GFP in a control (A, CZ333) and R13A5.9 mutant (B, CZ333 × TOG1) worm. (C) Distribution of full width at half maximum of fluorescent signal perpendicular to the dorsal nerve cord and fluorescence peak intensity in control (open circle, CZ333) and R13A5.9 mutant (closed circle, CZ333 × TOG1) worms. The full widths at half maximum and fluorescence peak intensity were obtained from the Gaussian curve fitting of fluorescence intensity along the crossline (white line in A). Scale bars represent 1 μm.

than that of CZ333 worms (600 ± 270 AU, n = 75). Collectively, these results suggested an excessive accumulation of synaptic vesicles in *R13A5.9* mutant worms.

4. Discussion

Through the generation of fusion proteins, we determined that R13A5.9 is expressed in or near synaptic vesicles, which suggested that this protein plays a role in synapse function in *C. elegans*. To explore the function of R13A5.9, *R13A5.9* mutant worms were generated through treatment with trimethylpsoralen and UV light. A potential loss-of-function mutation affecting *R13A5.9* was identified, and worms carrying this mutation were designated TOG1; TOG1 worms demonstrated several mutant phenotypes, including slow movement. Comparison of cholinergic pharmacology of TOG1 and wild-type worms suggested acetylcholine reception and postsynaptic response in TOG1 worms were normal. Importantly, TOG1 worms showed low sensitivity to aldicarb, which suggested that vesicular loading or release, or acetylcholine synthesis, was disrupted in these organisms. Furthermore, TOG1 worms demonstrated an excessive accumulation of synaptic vesicles. It is possible that defects in synaptic vesicle exocytosis in TOG1 worms may result in the accumulation of synaptic vesicles and disrupted acetylcholine release at neuromuscular junctions. Thus, our results suggest a functional role for R13A5.9 in synaptic vesicle exocytosis.

Although our results suggest a specific role for R13A5.9 in synapse function, it is likely that this protein is involved in other processes. Recently, it was reported that a mouse homolog of R13A5.9 (gi: 26338458), with 98 amino acid residues truncated from the N-terminus (Supplementary Fig. 1), is a receptor on macrophages that recognizes a major histocompatibility complex class I molecule [15]. Interestingly, this truncated region is conserved between mouse and *C. elegans*, and may alter the function of the resulting protein compared to homologs in other organisms. The *R13A5.9* mutant strain TOG1, developed during this study, might be useful for examining the effect of this truncation on the function of R13A5.9.

Acknowledgments

This work was supported by a Grant-in-Aid for an Academic Group Research Project (No. 14) from Iwate University. Some strains were provided by the CGC, which is funded by NIH Office of Research Infrastructure Programs (P40 OD010440).

Appendix A. Supplementary data

Supplementary data related to this article can be found at http://dx.doi.org/10.1016/j.bbrc.2015.06.048.

Transparency document

Transparency document related to this article can be found online at http://dx.doi.org/10.1016/j.bbrc.2015.06.048.

References

[1] *C. elegans* Sequencing Consortium, Genome sequence of the nematode C. elegans: a platform for investigating biology, Science 282 (1998) 2012–2018.
[2] S.K. Kim, J. Lund, M. Kiraly, et al., A gene expression map for *Caenorhabditis elegans*, Science 293 (2001) 2087–2092.
[3] K. Gengyo-Ando, S. Mitani, Characterization of mutations induced by ethyl methanesulfonate, UV, and trimethylpsoralen in the nematode *Caenorhabditis elegans*, Biochem. Biophys. Res. Commun. 269 (2000) 64–69.
[4] H. Inada, H. Ito, J. Satterlee, et al., Identification of guanylyl cyclases that function in thermosensory neurons of *Caenorhabditis elegans*, Genetics 172 (2006) 2239–2252.

[5] M.L. Nonet, Visualization of synaptic specializations in live *C. elegans* with synaptic vesicle protein-GFP fusions, J. Neurosci. Methods 89 (1999) 33–40.
[6] C. Mello, A. Fire, DNA transformation, in: H.F. Epstein, D.C. Shakes (Eds.), Caenorhabditis elegans: Modern Biological Analysis of an Organism, Academic Press Inc, San Diego, 1995, pp. 452–482.
[7] M.L. Nonet, O. Saifee, H. Zhao, et al., Synaptic transmission deficits in *Caenorhabditis elegans* synaptobrevin mutants, J. Neurosci. 18 (1998) 70–80.
[8] S.J. Hallam, Y. Jin, *lin-14* regulates the timing of synaptic remodeling in *Caenorhabditis elegans*, Nature 395 (1998) 78–82.
[9] P.E. Ash, Y.J. Zhang, C.M. Roberts, et al., Neurotoxic effects of TDP-43 overexpression in *C. elegans*, Hum. Mol. Genet. 19 (2010) 3206–3218.
[10] J.A. Lewis, J.T. Fleming, Basic culture methods, in: H.F. Epstein, D.C. Shakes (Eds.), Caenorhabditis elegans: Modern Biological Analysis of an Organism, Academic Press Inc., San Diego, 1995, pp. 4–29.
[11] L.A. Brown, A.K. Jones, S.D. Buckingham, et al., Contributions from *Caenorhabditis elegans* functional genetics to antiparasitic drug target identification and validation: nicotinic acetylcholine receptors, a case study, Int. J. Parasitol. 36 (2006) 617–624.
[12] C.H. Opperman, S. Chang, Effects of aldicarb and fenamiphos on acetycholinesterase and motility of *Caenorhabditis elegans*, J. Nematol. 23 (1991) 20–27.
[13] M.L. Nonet, J.E. Staunton, M.P. Kilgard, et al., *Caenorhabditis elegans rab-3* mutant synapses exhibit impaired function and are partially depleted of vesicles, J. Neurosci. 17 (1997) 8061–8073.
[14] O. Saifee, L. Wei, M.L. Nonet, The *Caenorhabditis elegans unc-64* locus encodes a syntaxin that interacts genetically with synaptobrevin, Mol. Biol. Cell. 9 (1998) 1235–1252.
[15] J. Tashiro-Yamaji, T. Kubota, R. Yoshida, Macrophage MHC receptor 2: a novel receptor on allograft (H-2D^dK^d)-induced macrophage (H-2D^bK^b) recognizing an MHC class I molecule, H-2K^d, in mice, Gene 384 (2006) 1–8.